Hardness and fracture toughness of dense calcium–phosphate-based materials

A. ŚLÓSARCZYK, J. BIAŁOSKÓRSKI
Faculty of Materials Science and Ceramics, University of Mining and Metallurgy, 30-059 Kraków, al. Mickiewicza 30, Poland

Hardness, H, and fracture toughness, K_{Ic}, have been determined as well as fracture energy and embrittlement index, H/K_{Ic} for six calcium–phosphate ceramics differing in phase composition. These materials were produced from initial calcium–phosphate precipitates with Ca–P molar ratios ranging between 1.50 and 1.73, synthesized by wet methods. After uniaxial or isostatic moulding and thermal treatment at 1250 °C, the obtained dense sinters constituted mono-, bi- or triphase ceramic materials containing hydroxyapatite (HAp), β-TCP, α-TCP and CaO. When comparing the investigated materials, the best parameters, i.e. relatively high hardness accompanied by high K_{Ic}, were observed in the case of a HAp–TCP composite, containing ~15 wt % HAp. It has been stated that free CaO occurring on the surface of the HAp samples obtained from powders with Ca–P ratios exceeding 1.67, transforms partially to $CaCO_3$ due to contact with the surrounding atmosphere. The well shaped calcite crystals existing on the surfaces of such sinters significantly reduce hardness and increase fracture energy of the material when comparing both with the monophase HAp and the biphase HAp–TCP ceramics.

1. Introduction

Among the calcium–phosphate-based ceramics, hydroxyapatite (HAp) and tricalcium phosphate (TCP), as well as HAp–TCP composites, are of greatest importance for medicine. These implantation materials are applied mainly in the field of dentistry and orthopaedy in the form of porous and dense blocks, granules and even as a powder [1, 2]. In general, in spite of their excellent biocompatibility, these brittle ceramics of limited mechanical strength are applied as osseous implants only at places not exposed to any significant mechanical load.

The investigations of calcium–phosphate materials include also an attempt to define the relationship between their phase compositions, microstructure and mechanical properties used as the parameters determining, in great measure, the application range.

Hardness, H, and toughness, K_{Ic}, are convenient material parameters for characterizing deformation and fracture phenomena in large scale of solids ranging from metals to ceramics. The H/K_{Ic} ratio combining hardness (resistance to deformation) and toughness (resistance to fracture) is used as a simple brittleness index [3].

In terms of fracture mechanics, the toughness parameter may be interpreted physically at two levels:

- macroscopically: it characterizes the combination of elastic and surface-formation properties;
- microscopically: it relates to the basic non-linear processes of separation responsible for crack-tip extension [4].

The former investigations regarded mainly the monophase HAp or TCP materials sintered in air at temperatures up to 1300 °C. These tests allowed the gathering of data on their microhardness and the hardness measured by Knoop or Vickers methods. The K_{Ic} values related to these materials have been determined mainly by three-point bending (single edge notched beam (SENB) geometry) [1, 5–9]. Using the Knoop method, Jarcho *et al.* [5] determined the hardness of dense polycrystalline HAp material sintered in air as equal to 4.8 GPa while the hardness of natural apatite reached ~ 4.3 GPa. The fracture toughness, K_{Ic}, of durapatite sintered at 1100–1200 °C for 1 h was 1.16 MPa $m^{1/2}$, i.e. one-third of that of alumina, while the fracture energy of both materials was nearly equal [7].

In general the fracture toughness and bending strength of TCP ceramics tend to be higher than those of HAp materials. The average K_{Ic} values of the toughest HAp and TCP samples sintered in air at a temperature ranging from 1000 to 1300 °C reached 0.96 and 1.30 MPa $m^{1/2}$, respectively [8]. The investigations carried out by Best *et al.* [9] revealed that the powder characteristics (surface area, grain size distribution) influenced significantly the sintering ability of dense HAp ceramics and determined the strength, hardness and fracture toughness of the final sinters. However, the optimum hardness and strength did not coincide with optimum fracture toughness for the series of powders and sintering temperatures investigated in their study.

The fracture toughness of the HAp ceramics can be improved by metal reinforcement. For the composites

containing 20 vol % metal fibres, De With and Corbijn [10] reached a K_{Ic} value six times higher compared with the base-line value (1.0 MPa $m^{1/2}$) for the pure HAp matrix. Simultaneously, the Knoop hardness and Young's modulus of such composites decreased (compared with the monophase HAp sinters) due to the lower hardness of the applied metal fibres reinforcement. Zhang *et al.* [11] used 30 vol % silver particles to reinforce the HAp bioceramics. It has been stated that the K_{Ic} value increased from 0.70 MPa $m^{1/2}$ for the base-line matrix, up to 2.45 MPa $m^{1/2}$ for the composite.

Similarly, the fracture toughness as well as the hardness could be improved by introducing another ceramic phase into the HAp matrix. Tagaki *et al.* [12] dispersed 26.8 wt % fine tetragonal zirconia polycrystal (TZP) powder in the HAp slurry. After sintering the fracture toughness of the materials obtained was approximately 100% higher than that of the HAp matrix. On the other hand, the reinforcement of the HAp matrix with SiC platelets (up to 15 vol %) causes an increase in Vickers hardness by up to 30% [13]. When comparing the value $K_{Ic} = 0.96$ MPa $m^{1/2}$ reported for the monophase HAp material, the fracture toughness of titanium dioxide doped HAp ceramics increases up to 1.95 MPa $m^{1/2}$ [14].

Kijima and Tsutsumi [15] investigated dense polycrystalline oxyhydroxyapatite bodies and found that the change of sintering temperature from 1050 to 1350 °C caused an increase of Vickers microhardness from 5.2 up to 6.5 GPa. For 1450 °C a slight decrease in microhardness has been observed. The average Vickers microhardness obtained for the apatite samples sintered to $>98\%$ theoretical density was ~6.4 GPa, while for natural apatite this reached 7.4 GPa. The microhardness of tooth enamel equal to ~3.4 GPa is lower than that reached for the HAp bioceramics sintered up to 97–99.9% relative density (4.5 GPa) [1].

The systematical study carried out by Van Landuyt *et al.* [16] proved the effect of sintering temperature on fracture toughness and hardness of HAp ceramic materials sintered in air at temperatures up to 1450 °C. An increase of K_{Ic} from 0.67 to 0.97 MPa $m^{1/2}$, i.e. by 40%, has been observed for sintering temperatures ranging from 1000 to 1300 °C. Simultaneously, the hardness of these specimens increased by over 200%. Further increase of hardness has been stated for higher sintering temperatures (up to 1400 °C).

Wang and Chaki [17] reported the effect of the sintering process atmosphere on the dissociation of HAp and mechanical properties of the final materials. Due to the decomposition of HAp at relatively low sintering temperatures, the Knoop hardness of HAp blocks sintered in vacuum was always lower (~1.6 GPa) than that of HAp sintered in air (~2.0 GPa) at corresponding temperatures. The lowest values were obtained for HAp material sintered in humid air (~0.3 GPa).

This work was aimed at the determination of Knoop hardness and K_{Ic} of six calcium–phosphate materials obtained from apatite precipitates with differing Ca–P molar ratios. The relationship between the hardness as well as K_{Ic} values of these sinters and their phase compositions were determined.

2. Materials and methods

2.1. Processing of the samples

Six calcium–phosphate precipitates of different Ca–P molar ratio have been prepared following a wet procedure, using CaO and H_3PO_4 as substrates. The proportion of $Ca(OH)_2$ suspension and H_3PO_4 solution as well as the pH of the reaction medium controlled by the application of aqueous solution of ammonia (1 : 1) were used as variable parameters determining the synthesis conditions.

The precipitates were aged for 48 h at room temperature, then filtered, dried at 90 °C and ground in a rotating-vibrating mill. The powders were calcined at 800 °C for 3 h, mixed with a 5 wt % solution of polyvinyl alcohol and compacted uniaxially under a pressure of 150 MPa to form parallelepipedic bars of $80 \times 80 \times 5$ mm final size. A second group of compacts was obtained as a result of initial uniaxial pressing followed by isostatic repressing under 350 MPa.

The sintering process involved heat treatment in air at 1250 °C with a 2 h soaking time. The rate of temperature increase was 100 °C h^{-1} and cooling was carried out together with the furnace. As a reference base-line, the samples prepared from the commercial HAp powder manufactured by Merck have been sintered simultaneously (AM samples).

2.2. Methods

The content of calcium and phosphorus in the initial powders was determined by chemical analysis, i.e. using $KMnO_4$ titration for calcium and the phosphomolybdate procedure for phosphate determination. The bulk density of the sintered bodies was tested using a ACCU-PYC 1330 helium pycnometer. The phase composition of the sinters was determined by the X-ray powder diffraction method using a Philips diffractometer. The fracture surfaces were investigated by scanning electron microscopy (SEM, Jeol-5400). The carbon concentration in the CaO-containing samples was estimated by the energy dispersive spectroscopy (EDX) method (Link AN 10 000). Non-destructive ultrasonic investigations were used to determine the Young's modulus following the method described by Piekarczyk *et al.* [18].

2.3. Knoop hardness tests

The surfaces of samples used in hardness and fracture toughness tests were ground, polished with abrasive papers (No. 400–1200) and with fabric soaked with water suspension of alumina powder (1200). The final treatment was performed on a beech polishing wheel with 1 μm diamond paste. Such a procedure led to the removal of a ~1 mm thick layer to avoid the "skin" effect on mechanical properties of the internal part of the sinter. At least five Knoop indentations were performed with a load ranging from 2 to 20 N in order to investigate the hardness. The Vickers method has not

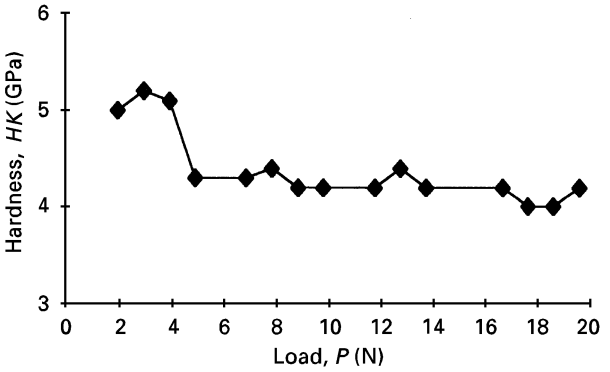

Figure 1 Knoop hardness versus load for the sample of A4 material uniaxially pressed.

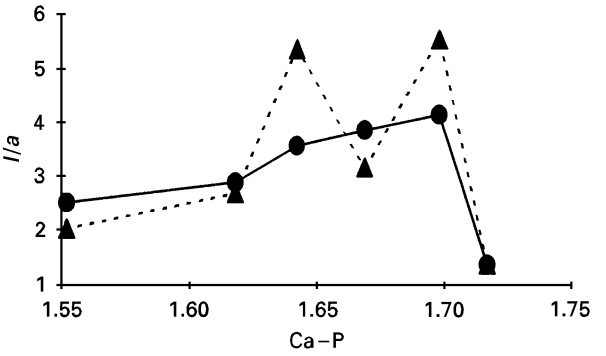

Figure 2 The l/a coefficient as a function of Ca–P ratio of the initial powder: (–●–) uniaxial load, (–▲–) isostatic load.

been used because of cracking observed in indentation edges even in the case of the lowest load (1.96 N).

A typical dependence of Knoop hardness as a function of load is shown in Fig. 1 for the A4 sample. Usually the hardness is higher for lower loads (2–10 N) and it decreases or remains constant for higher loads (up to 20 N). Therefore the Knoop hardness of investigated materials has been calculated as an average value within the range of its smaller variability.

2.4. Fracture toughness tests

The Vickers indentation of brittle calcium-phosphate materials causes the creation of crack patterns that can be described mainly according to the median crack system. It has been confirmed when analysing the relationship between crack length, l, and load, P, as well as using the l/a ratio analysis for a chosen load. For the median cracks

$$c = A \times P^{(2/3)} \tag{1}$$

where $c = a + l$, and a is the half-diagonal of the Vickers indent; and A is a constant.

The investigations carried out for the A2 sample within the load range from 1.96 to 88.29 N allowed estimation of the exponent value to be 2/5 (the correlation coefficient being 0.92). The values 2/3 and 2/5 differ considerably and therefore the better arguments are obtained from the l/a versus Ca–P ratio dependence (Fig. 2) measured for the chosen load (P = 29.43 N). For all the samples (excluding A6; Ca–P = 1.73; $l/a = 1.4$) it follows that $l/a \geq 2$ and therefore the fracture toughness, K_{Ic}, is calculated using Equation 2, which is related to the median cracks [19]

$$K_{Ic} = 0.016 \times \left(\frac{E}{H}\right)^{0.5} \times \left(\frac{P}{c^{1.5}}\right) \tag{2}$$

In the case of the A6 sample, for which $l/a = 1.4$, the K_{Ic} parameter is calculated using the Palmqvist crack formula [20]

$$\frac{K_{Ic} \times \phi}{H \times a^{0.5}} \times \left(\frac{H}{E \times \phi}\right)^{0.4} = 0.035 \times \left(\frac{1}{a}\right)^{-0.5} \tag{3}$$

where H is the hardness, E is Young's modulus, and ϕ is the coefficient related to the material constraint ($\phi \cong 3$).

The five–six Vickers indentations were made at a load $P = 24.93$ N applied for 15 s (in a manner similar to the Knoop indentations) using a Zwick 3 212 000 hardness tester. The lengths of the indentations were measured with a microscope in reflected light at $\times 500$–1000 magnification. This procedure of K_{Ic} determination led to slight under estimation of fracture toughness comparing with the results obtained using the three-point notched beam tests [11, 21].

3. Results and discussion

Among the precipitates obtained in consecutive syntheses there is a single one (the powder precursor No. 4) that shows a Ca–P ratio equal to 1.67 (Table I), i.e. corresponding with the stoichiometric HAp composition. In the case of three other precipitates Ca–P ratios less than 1.67 were found, while for the remaining two the values were above 1.67.

After sintering at 1250 °C the dense materials were produced. In the case of the samples uniaxially compacted, their relative densities ranged between 95.9 and 99.6% and for the isostatically repressed samples, from 98.0 to 99.9% (Fig. 3).

TABLE I Ca–P molar ratios of the initial precipitates

Sample No.	1	2	3	4	5	6	7
Ca–P ratio	1.50	1.55	1.61	1.67	1.70	1.73	1.64

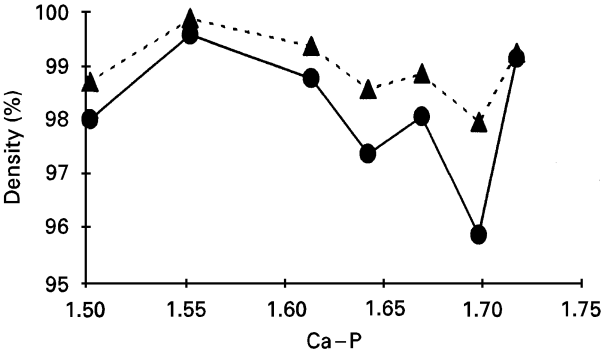

Figure 3 Relative densities of the sinters versus Ca–P ratios of the initial powders: (–●–) uniaxial load, (–▲–) isostatic load.

TABLE II Phase composition of calcium–phosphate materials after sintering at 1250 °C

	A1	A2	A3	A4	A5	A6	AM
HAp, wt %	0	15	60	100	≤ 99	≤ 98	97
β-TCP, wt %	70	75	35	0	0	0	3
α-TCP, wt %	30	10	5	0	0	0	0
CaO, wt %	0	0	0	0	≥ 1	≥ 2	0

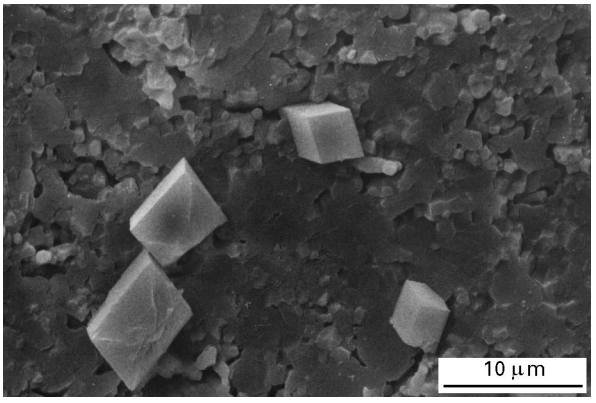

Figure 4 Microstructure of the A6 HAp material with well shaped calcite crystals.

The qualitative XRD studies showed significant variability of phase composition of the investigated materials (Table II). After heat treatment at 1250 °C the sinters were mono-, bi- and triphase ceramics consisting of HAp, β-TCP, α-TCP and CaO.

A monophase HAp ceramic has been obtained only from the precipitate with a Ca–P ratio equal to 1.67 (sample A4), while the sinter obtained from the powder precursor with a Ca–P ratio equal to 1.50 consisted of β-TCP and α-TCP (sample A1). The initial precipitates characterized by a Ca–P ratio greater than 1.67 form after sintering the HAp materials containing up to ~2 wt % CaO (samples A5 and A6). The other two investigated samples were HAp–TCP ceramic materials containing up to 60, 75 and 10 wt % HAp, β-TCP and α-TCP, respectively.

The SEM observations and EDX studies have confirmed that the CaO occurring on the fracture surfaces of the samples manufactured from the initial powders with a Ca–P ratio greater than 1.67, transforms in air to form $Ca(OH)_2$ and then, partially, to $CaCO_3$. Former Fourier transform infrared investigations [22] have shown that the band at $\sim 3642\,cm^{-1}$ corresponding to the vibrations of the OH^- group contained in the calcium hydroxide is more intensive in the case of sample A6. It indicates that there is a greater content of this phase in sample A6 than in sample A5.

In the case of sample A6 (Fig. 4) well shaped calcite crystals were detected on its fracture surfaces, while sample A5 contained only fine $CaCO_3$ aggregates (Fig. 5).

The microstructure of the investigated materials is diverse. The best sintered, almost pore-free samples have been obtained in the case of mono-phase HAp bioceramics (sample A4; Fig. 6). The highest quantities

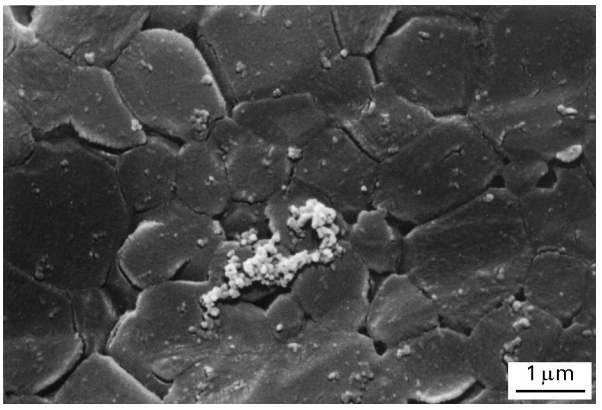

Figure 5 Microstructure of the A5 HAp material with fine $CaCO_3$ crystals.

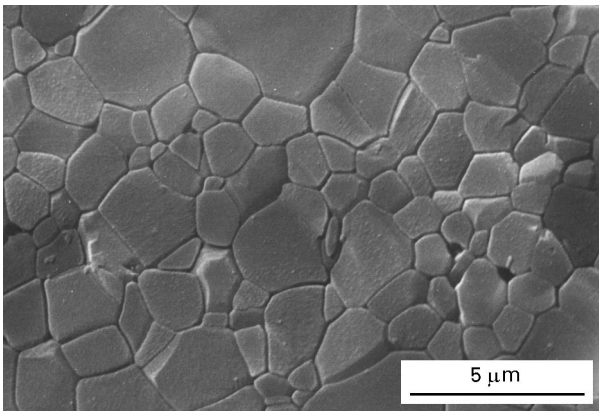

Figure 6 Microstructure of monophase HAp material (sample A4).

of pores and fractures have been observed on fractured surfaces of ceramics with TCP as the major component (samples A1 and A2). It is probably due to the worse sinterability of TCP powders [5] as well as a result of stress connected with the polymorphous transformation of β-TCP ↔ α-TCP and with the difference in thermal expansion coefficients of coexisting phases [23].

The results of hardness measurements given in Tables III and IV and presented graphically in Fig. 7 indicate that, except for sample A6, the hardnesses of all the sinters are similar, ranging between 4.0 and 4.9 GPa. The Knoop hardness values of the A6 ceramics are significantly lower (by ~35%). This material contains HAp as the dominating phase as well as ~2 wt % CaO. Such a significant reduction of hardness may be related to the occurrence of well shaped calcite crystals on the surface. These crystals were formed due to contact of sample A6 with the environment containing H_2O and CO_2. The hardness of calcite according to Mohs' scale is three, compared with five for apatite.

The isostatic repressing of the samples did not influence the hardness of the investigated materials, in comparison with the uniaxially pressed compacts. In the case of sample A1, the measurements were not feasible due to the cleavage of this material. Because of the special procedure of K_{Ic} determination applied in this work, giving slightly underestimated (by ~15%)

TABLE III Mechanical properties of calcium–phosphate materials, uniaxially pressed

No.	H (GPa)	K_{Ic} (MPa m$^{0.5}$)	E^a (GPa)	γ^b (J m^{-2})	H/K (μm$^{-0.5}$)
A2	4.2 ± 0.1	1.24 ± 0.16	93 ± 3	8.3	3.4
A3	4.3 ± 0.1	0.76 ± 0.21	95 ± 2	3.0	5.7
AM	4.0 ± 0.1	0.64 ± 0.08	98 ± 5	2.1	6.2
A4	4.2 ± 0.1	0.57 ± 0.09	103 ± 2	1.6	7.4
A5	4.1 ± 0.2	0.52 ± 0.08	96 ± 1	1.4	7.9
A6	2.6 ± 0.1	1.22 ± 0.16	68 ± 1	10.9	2.1

[a] Young's modulus was determined by the ultrasonic method.
[b] Fracture energy was calculated according to the formula $\gamma = K_{Ic}^2/2E$.

TABLE IV Mechanical properties of calcium–phosphate materials, isostatically repressed

No.	H (GPa)	K_{Ic} (MPa m$^{0.5}$)	E^a (GPa)	γ^b (J m^{-2})	H/K (μm$^{-0.5}$)
A2	4.6 ± 0.3	1.28 ± 0.12	102 ± 1	8.0	3.6
A3	4.9 ± 0.3	0.99 ± 0.13	104 ± 1	4.7	4.9
AM	4.2 ± 0.4	0.44 ± 0.06	107 ± 1	0.9	9.5
A4	4.6 ± 0.3	0.73 ± 0.24	109 ± 3	2.4	6.3
A5	4.0 ± 0.3	0.41 ± 0.05	109 ± 1	0.8	9.8
A6	2.7 ± 0.2	1.32 ± 0.15	77 ± 1	11.3	2.0

[a] Young's modulus was determined by the ultrasonic method.
[b] Fracture energy was calculated according to the formula $\gamma = K_{Ic}^2/2E$.

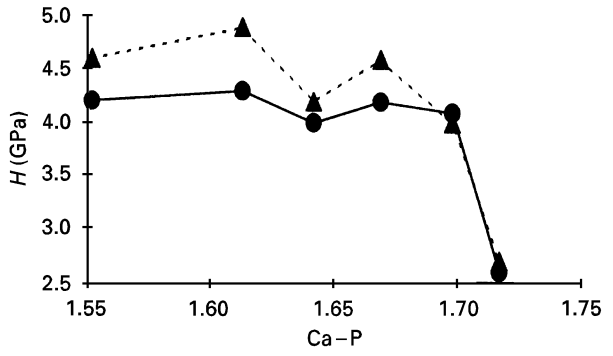

Figure 7 Knoop hardnesses of the sinters versus Ca–P ratios of the initial powders: (–●–) uniaxial load, (–▲–) isostatic load.

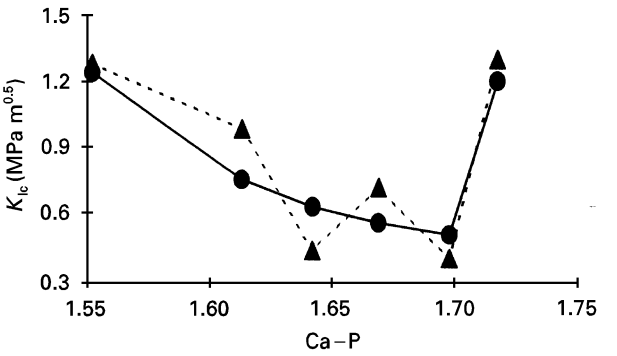

Figure 8 Fracture toughnesses of the sinters versus Ca–P ratios of the initial powders: (–●–) uniaxial load, (–▲–) isostatic load.

results in relation to the more popular SENB method, it seems difficult to compare the obtained data with those quoted in literature. However, the results obtained for separate calcium–phosphate materials with different phase compositions are comparable for sure.

Fig. 8 illustrates the dependence of K_{Ic} as a function of Ca–P ratio of the initial powders, and Tables III and IV present the values of K_{Ic}, fracture energy, Young's modulus and brittleness indices H/K_{Ic}, for the investigated materials (except for sample A1).

It results from the data presented, in the case of a monophase HAp ceramic material, that K_{Ic} for the samples formed uniaxially and isostatically is equal to 0.57 and 0.73 MPa m$^{1/2}$, respectively.

The value of K_{Ic} parameter of the A2 sinters, a biphase ceramic material containing $\sim$15 wt % HAp and $\sim$85 wt % TCP, is two times higher than that of monophase HAp. In the case of uniaxially or isostatically repressed samples, the K_{Ic} values reach 1.24 and 1.28 MPa m$^{1/2}$, respectively. The increase of HAp content (sample A3) up to 60 wt % causes a decrease of the K_{Ic} parameter; nevertheless it is still higher by $\sim$30–40% than in the case of monophase HAp ceramics.

K_{Ic} for sample A2 is relatively high. Its fracture energy is also high ($\sim$8 J m^{-2}) when comparing it with all the investigated samples. On the other hand, the brittleness indices, H/K_{Ic}, are relatively low, 3.4 and 3.6 μm$^{-0.5}$, respectively.

Investigations carried out by Aoki and coworkers [2, 6] and by Royer *et al.* [24] prove that the best mechanical results are obtained for a HAp containing a TCP composite, whereas for near pure HAp the flexural strength decreases. It is suggested that the strengthening of HAp by TCP involves surface compression due to the β-TCP ↔ α-TCP transformation [24].

Results obtained in this study indicate that the fracture toughness and fracture energy of the biphase TCP–HAp materials are higher than in the case of pure monophase HAp. When comparing the mechanical properties of a composite with predominant

tricalcium phosphate (the HAp content being ~15 wt %) and another material with predominant HAp phase (~60 wt %) it appears that an improvement of the fracture toughness is observed for a lower HAp content.

Relatively high K_{Ic} values (close to those observed for TCP–HAp composites), have been measured for sample A6. This sample also showed the highest fracture energy (~11 J m^{-2}) and the lowest brittleness index (~2 μm$^{-0.5}$). Furthermore, when compared with other samples, this material had significantly lower Young's modulus (68 GPa, for uniaxially pressed samples, and 77 GPa, for isostatically compacted ones).

Interpretation of the results obtained for HAp ceramic materials containing CaO as a secondary phase seems to be more complex. It is well known that the CaO phase existing in the HAp material causes reduction in its bending strength [24]. It probably results from CaO hydration, which is known to build up stress due to the greater volume of the resultant hydroxide.

In our research, the CaO phase existing as a secondary phase influences the reduction of Young's modulus in sample A6, compared with pure HAp and HAp–TCP composites. This regularity has not been found in the case of sample A5. It can be explained taking into consideration the smaller grain size and smaller content of free CaO phase in the latter material. It may be expected, based upon the morphological observations (Figs 4 and 5) and upon the quantity of $CaCO_3$ crystals formed on the surfaces of samples A5 and A6. The relatively high K_{Ic} values for sample A6 can be explained by the formation of well shaped calcite crystals on its surface. It corresponds with the Palmqvist cracking that occurs in this material. It is well known that such cracks are developed at relatively small depth (~9.5 μm in this case) under the surface of the sample and they may be inhibited by relatively large (~10 μm wide) $CaCO_3$ crystals formed on the surface that are poorly connected with the matrix. It influences the reduction of the measured length of the cracks, l, and, consequently, it causes a probable increase of the K_{Ic} value.

4. Conclusions

1. The mono-, bi- and triphase calcium–phosphate materials containing HAp, β-TCP and α-TCP, produced from precipitates with Ca–P molar ratios ≤ 1.70 show similar values of hardness in the range 4.1–4.9 GPa.

2. The highest K_{Ic} value in relation to the monophase HAp ceramics revealed a TCP–HAp composite material containing ~15 wt % HAp.

3. About 2 wt % CaO as a secondary phase in HAp materials sintered from an initial precipitate with a Ca–P ratio equal to 1.73 significantly reduces the Young's modulus of the body. Free CaO occurring on the fracture surfaces of the samples transforms in air to $CaCO_3$. Well shaped calcite crystals cause the reduction of material hardness by ~35%. Probably their inhibitory influence on the development of Palmqvist cracks results in increasing fracture toughness of the ceramics.

Acknowledgements

The authors thank Dr Jan Piekarczyk for performing measurements and for calculation of the Young's modulus as well as for discussion of the results.

References

1. A. RAVAGLIOLI and A. KRAJEWSKI, In "Bioceramics: materials, properties, applications" (Chapman & Hall, London, 1992) pp. 173–93 and 310–13.
2. H. AOKI, In "Medical applications of hydroxyapatite" (Ishiyaku Euro-America, Tokyo, 1994) pp. 90–173.
3. B. R. LAWN and D. B. MARSHALL, *J. Amer. Ceram. Soc.* **62** (1979) 347.
4. B. R. LAWN and T. R. WILSHAW, In "Fracture of brittle solids" (Cambridge University Press, London, 1975) Ch. 3 and 4.
5. M. JARCHO, C. H. BOLEN, M. THOMAS, J. BOBICK, J. KAY and R. DOREMUS, *J. Mater. Sci.* **11** (1976) 2027.
6. A. AOKI, K. KATO, M. OGISO and T. TABATA, *Shika-Tenbö* **49** (1977) 567.
7. M. B. THOMAS and R. H. DOREMUS, *Amer. Ceram. Soc. Bull.* **60** (1981) 258.
8. M. AKAO, N. MIURA and H. AOKI, *Yogyo-Kyokai-Shi* **92** (1984) 672.
9. S. BEST, W. BONFIELD and C. DOYLE, In Proceedings of the second International Symposium on Ceramics in Medicine, Heidelberg, Germany, September 1989, edited by G. Heimke, pp. 57–64.
10. G. DE WITH and A. J. CORBIJN, *J. Mater. Sci.* **24** (1989) 3411.
11. X. ZHANG, G. H. M. GUBBELS, R. A. TERPSTRA and R. METSELAAR, In Fourth Euro Ceramics, Vol. 3, edited by S. Meriani and V. Sergo, Faenza (1995) pp. 287–92.
12. M. TAGAKI, M. MOCHIDA, N. UCHIDA, K. SAITO and K. UEMATSU, *J. Mater. Sci. Mater. Med.* **3** (1992) 191.
13. T. NOMA, N. SHOJI, S. WADA and T. SUZUKI, *J. Ceram. Soc. Jap.* **100** (1992) 1175.
14. A. ŚLÓSARCZYK, M. AKAO, H. AOKI and S. NAKAMURA, *MRS Int'l Mtg. on Adv. Mats, Materials Research Soc.*, vol. 1 (1989) 317–322.
15. T. KIJIMA and M. TSUTSUMI, *J. Amer. Ceram. Sci.* **62** (1979) 455.
16. P. VAN LANDUYT, F. LI, J. P. KEUSTERMANS, J. M. STREYDIO, F. DELANNAY and E. MUNTING, *J. Mater. Sci. Mater. Med.* **6** (1995) 8.
17. P. E. WANG and T. K. CHAKI, *ibid.* **4** (1993) 150.
18. J. PIEKARCZYK, H. K. HENNICKE and R. PAMPUCH, *CFJ/Ber DKG* **59** (1982) 227.
19. G. R. ANSTIS, P. CHANTIKUL, B. R. LAWN and D. B. MARSHALL, *J. Amer. Ceram. Soc.* **64** (1981) 533.
20. K. NIIHARA, R. MORENA and D. P. H. HASSELMAN, *J. Mater. Sci. Lett.* **1** (1982) 13.
21. J. BIAŁOSKÓRSKI and J. PIEKARCZYK, Unpublished data.
22. A. ŚLÓSARCZYK, C. PALUSZKIEWICZ, M. GAWLICKI and Z. PASZKIEWICZ, **23** (1997) 297.
23. G. BAUER, In "Biokeramik als Implantatwerkstoff für die Humanmedizin" (Erlangen, 1988) pp. 56–93 and 151.
24. A. ROYER, J. C. VIGUIE, M. HEUGHEBAERT and J. C. HEUGHEBAERT, *J. Mater. Sci. Mater. Med.* **4** (1993) 76.

Received 19 April 1996
and accepted 1 September 1997